Spatially Resolved and Highly Complexed Protein and RNA *in situ* Detection by Combining CODEX with RNAscope In Situ Hybridization

Yilun Cheng,[1, 2] Rachel K. Burrack[1, 2] and Qingsheng Li[1, 2] *

[1]Nebraska Center for Virology, [2]School of Biological Sciences, University of Nebraska-Lincoln, Lincoln, NE 68583.

*Corresponding author: Mailing address: Nebraska Center for Virology, School of Biological Sciences, University of Nebraska-Lincoln, Morrison Center P.O. Box 830666, Lincoln, NE 68583-0900

Phone: (402) 472-5922; E-mail: qli@unl.edu

Running Head: highly complexed CODEX and RNAscope ISH combination

ABSTRACT

Highly multiplexed protein and RNA *in situ* detection on a single tissue section concurrently is highly desirable for both basic and applied biomedical research. CODEX is a new and powerful platform to visualize up to 60 protein biomarkers in situ and RNAscope in situ hybridization (RNAscope) is a novel RNA detection system with single-copy sensitivity and unprecedent specificity at a single cell level. Nevertheless, to our knowledge, the combination CODEX and RNAscope remained unreported until this study. Here we report a simple and reproducible

combination of CODEX and RNAscope (Comb-CODEX-RNAscope) . We also determined the cross-reactivities of CODEX anti-human antibodies to rhesus macaques, a widely used animal model of human disease.

INTRODUCTION

Highly multiplexed protein *in situ* detection (HMPISD) on a single tissue section at subcellular resolution is a powerful new technology to visualize and quantify proteins in their native tissue microenvironment with spatial context (1-3). The HMPISD technologies have been wildly used in basic and applied biological research. The HMPISD has also been used in cancer biology to explore the complex immune landscapes and tumor microenvironment (1, 3-7) and in the study of pathogenesis of autoimmune disease (8). Several strategies and platforms of HMPISD have been developed and utilized including 1) Time-of-Flight Mass Spectrometry based platforms of Imagine Mass Cytometry (IMC) (9, 10) and Multiplexed Ion Beam Imaging (MIBI) (11, 12). Both methods combined metal-labeled antibody immunostaining, UV laser ablation in IMC or ion beam gun ablation in MIBI, and CyTOF mass cytometry; 2) iterative fluorescent-conjugated antibody staining, imaging, and removing antibody or inactivating fluorophores. For example, MultiOmyx (13-15) and the tissue-based CyClic ImmunoFluorescence (t-CyCIF) (16, 17); and 3) DNA-barcoded antibody platforms. For example, the Immunostaining with Signal Amplification by Exchange Reaction (Immuno-SABER) (18, 19) and CO-Detection by inDEXing (CODEX). In Immuno-SABER, tissue target proteins are first bound with a panel of DNA-conjugated antibodies, subsequently multiple rounds of hybridizing with corresponding concatemer DNA and fluorescent-DNA, imaging, and removing the fluorophores. CODEX is a new and powerful platform, of which multiple epitopes are first bound with a panel of barcoded oligonucleotide conjugated antibodies followed by multiple cycles of adding corresponding fluorescently labeled-oligonucleotide probes, imaging, and removing fluorescently-labeled-oligonucleotide probes to

visualize up to 60 protein biomarkers *in situ* (6, 8, 20). While the prototype CODEX using dNTP analogs plus DNA polymerase primer extension to amplify signal of DNA barcode conjugated to antibody (8), the current CODEX uses chaotropic solvents to facilitate sequential room temperature (RT) annealing and stripping process without polymerase reaction (6). Compared to other HMPISD methods, CODEX enlarges multiplexing ability (3, 20), increases detection resolution to subcellular level(1), preserves tissue architecture, and reduces experiment duration through single staining procedure(1). Simultaneous visualization of spatially resolved highly multiplexed proteins and RNA *in situ* is highly desirable for both basic and applied biomedical research(21, 22). RNAscope *in situ* hybridization (RNAscope) from Advanced Cell Diagnostics (ACD) is a novel RNA detection system with single-copy sensitivity and unprecedent specificity at a single cell level (19, 23). Nevertheless, RNAscope and CODEX involve complex chemical and physical procedures. To our knowledge, the combination CODEX and RNAscope (Comb-CODEX-RNAscope) remained unknown until this study.

In this study, we tested various methods of combination and found a simple and reproducible approach of CODEX first and RNAscope second (Comb-CODEX-RNAscope) to visualize highly complexed proteins and RNA simultaneously in a single tissue section. Currently, highly multiplexed protein *in situ* detection platforms including CODEX is designed for human sample detection using anti-human antibodies. Non-human primates evolutionally, anatomically, and physiologically are the closest species to humans and are regarded as one the best animal models of many human diseases. Nevertheless, the CODEX antibody compatibility to NHP was unknow until this study. We therefore determined the cross- reactivities of CODEX anti-human antibodies to rhesus macaques, which are the most widely used NHP to model human diseases including HIV (24, 25).

RESULTS

Determine the cross-reactivities of CODEX anti-human antibodies to rhesus macaques

To determine the cross- reactivities of CODEX anti-human antibodies to rhesus macaques, a panel of DNA-barcoded anti-human antibodies from Akoya Biosciences (Akoya) was tested in various fixative fixed (SafeFixII, 4% Paraformaldehyde, neutral-buffered formalin) and paraffin embedded lymph node tissues of rhesus macaques who were infected with SIV. We found 13 out of 24 CODEX anti-human antibodies from Akoya were reactive specifically with rhesus macaques (**Table 1 & Fig 1**). The DNA-barcoded anti-human CD3 antibody from Akoya (CD3e, Clone# EP449E) did not react with rhesus macaque tissues. We therefore conjugated another anti-human CD3 antibody (SP162, Cat#: ab245731, Abcam) with a DNA-barcoded oligonucleotide (Cat#: 5350002, Akoya) by following the conjugating kit manual (Cat#: 7000009, Akoya). After verifying the size was correct through protein gel electrophoresis, the conjugated CD3 antibody was tested using CODEX. It worked well for rhesus macaque tissues, where CD3 signals were clearly separated from CD20 signals and partially colocalized with CD4 signals and primarily distributed in T cell zone of lymph node tissues (**Fig 2**).

The Combination of CODEX immunostaining with RNAscope ISH

After identifying rhesus macaque compatible antibodies, we selected a subset of them that are important for SIV immunopathogenesis to test various methods of combining CODEX with RNAscope. Two different orders of combination, RNAscope and subsequent CODEX as well as CODEX and subsequent RNAscope, were tested. All the procedures including deparaffinization, tissue hydration and antigen retrieval were conducted to minimize RNase contamination. RNAscope and subsequent CODEX method significantly induced non-specific signals and reduced the specific signals of CODEX. This combination led to unaccepted low signal-noise-

ratio (SNR) of CODEX as compared with a single CODEX, although RNAscope signals maintained before and after CODEX (data not shown). Since RNAscope and subsequent CODEX approach could not get satisfying results, next efforts were focused on the approach of CODEX and subsequent RNAscope. When following the protocol of single CODEX and single RNAscope sequentially, RNAscope signals could not consistently detected, although CODEX signal detection worked well. It was plausible that some steps of CODEX including the antigen-retrieval step might impair RNAscope signal detection. It was tested and excluded the impact of number of cycles of CODEX on the RNAscope signal detection by comparing single cycle vs multiple cycles of CODEX immunostaining. It was further excluded the impact of RNase contamination of CODEX fluidics instrument by adding CODEX fluidics washing step into a single RNAscope procedure. The washing with CODEX fluidics did not impact RNAscope signal detection. It was

narrowed down that the source of inconsistent RNAscope signal detection was in the antigen-retrieval step using a high-pressure cooker (Decloaking Chamber™, Biocare Medical). An alternative method for antigen retrieval using 50 ml glass-beaker on a Hotplate (Thermo Fisher, SP88857104) was tested, where the coverslips with tissue sections were placed in the coverslip staining rack (PN# 72240, Electron Microscopy Science) and immersed in boiling citrate buffer (pH 6, Sigma 21545) for 20 min. This method is simple and easy to eliminate potential RNase contamination by pre-baking glass-beaker and coverslip staining rack covered with aluminum foil at 300 ^{o}C for 6 hrs. The developed CODEX and subsequent RNAscope approach (Comb-CODEX-RNAscope) with hotplate antigen retrieval is simple and reproducible for both highly multiplexed protein and RNA detections for SafeFixII, 4% paraformaldehyde, and neutral-buffered formalin fixed and paraffin-embedded tissues (**Fig 3**). SIV viral RNA (vRNA) signals from RNAscope (**Fig 4B-C**) in addition to CD3, CD4 CD68, CD20, CD21, CD31, HLA-DR , Ki67

and DAPI from CODEX (**Fig 4D-L**) are specific and intense enabling downstream spatial analyses.

MATERIALS AND METHODS

Rhesus Macaque Tissues

Archived fixed lymphatic tissues from adult rhesus macaques infected with SIVmac251 from our previous reported studies were used(26, 27). Rhesus macaques were intra-rectally inoculated with SIVmac251 (3.1 x 10^4 $TCID_{50}$) and were euthanized at different days post-inoculation and rhesus macaques without virus inoculation served as uninfected controls. Lymph node tissues were fixed with SafeFix II (Cat# 23-042600, Fisher Scientific), 4% paraformaldehyde or neutral-buffered formalin and embedded with paraffin.

Antibody-oligonucleotide conjugation:

To find a rhesus macaque reactive CD3 antibody for CODEX, an anti-human CD3 antibody in a carrier-free PBS solution (Clone#: SP162, Cat#: ab245731, Abcam) was conjugated with the barcode-oligonucleotide (Cat#: 5350002, Akoya) using CODEX conjugation kit (Cat#: 7000009, Akoya) following CODEX conjugation manual.

CODEX immunostaining

CODEX immunostaining was performed according to CODEX user manual and previously published method (20). Six-µm tissue sections were cut using Leica RM2235 rotary microtome and mounted to poly-lysine coated coverslips. The following steps were performed in 6-well

tissue culture plate. Tissue-coverslips were deparaffinized by sequentially heating on a hotplate at 60°C for I hr and immersed in xylene for 5 min twice and rehydrated with gradually decreased concentration of ethanol and DEPC water. The antigen retrieval was performed in a high-pressure cooker (Decloaking Chamber™, Biocare Medical) for 20 min at high-pressure or Hotplate (Thermo Fisher, SP88857104) boiling for 20 min. The tissue-coverslips in the coverslip staining rack (PN# 72240, Electron Microscopy Science) were immersed in citrate buffer (pH 6, Sigma 21545) in 50 ml glass beaker. After antigen retrieval, the tissue-coverslips were stained with a cocktail of DNA-barcoded antibodies for 3 hrs at room temperature (RT). After washing in PBS 3 times, 2 min each to remove unbound antibodies, the tissue-coverslips were post-fixed with 1.6% PFA for 10 min at RT, washed, post-fixed with ice-cold methanal for 5 min and washed. The tissue-coverslips then could be stored in the storage buffer for 5 days at 4°C or immediately loaded into CODEX instrument for multiple cycle immunostaining. The CODEX fluidics and Keyence microscope was set up using CODEX instrument manager (CIM) software and Keyence software according to manufacturer's protocol. The master mix of fluorescently-labeled-oligonucleotide probes (fluorescent-reporters) that corresponded to DNA-barcoded antibodies for multiple cycle immunostaining was prepared in a 96-well plate according to CODEX manual. Each cycle of CODEX immunostaining consisted of three steps of adding nuclear staining DAPI, Atto550-, Cy5- and Cy7-fluorescent-reporters, imaging, and removing fluorescent-reporters. Two blank cycles (DAPI nuclear stain only and without any fluorescent-reporters) were ran for evaluating the level of autofluoresence and subtracting background using CODEX processor software.

RNAscope ISH

RNAscope ISH (RNAscope) was performed according to the manufacturer's protocol and our previously published method(28, 29) with slight modifications. All the procedures including deparaffinization, hydration and antigen retrieval were conducted to minimize RNase contamination. The tissue-coverslips were deparaffinized and rehydrated as described in the CODEX section above and incubated in 3% hydrogen peroxide for 10 min at RT. After Washing in mili-water (AQUA SOLUTION, 2700PRD), the tissue-coverslips were subjected to antigen retrieval by boiling for 15 min in RNAscope® Target Retrieval Reagent solution (Cat # 322000, ACD) in a 50ml glass beaker on Hotplate to undo the cross-linking. After treatment with RNAscope® Protease Plus (Cat # 322330, ACD) at 40°C for 20 min, tissue-coverslips were hybridized with RNAscope® Probe- SIVmac239 (anti-sense, Cat# 312811, ACD) at 40°C for 2 hrs. The signals were amplified and detected with RNAscope® 2.5 HD assay-Red kit (Cat# 322360, ACD), where the fast red can be visualized both in regular light and in far-red fluorescent channel. The RNAscope® negative control probe-DapB (Cat# 310043, ACD) was used as negative control.

Combination of CODEX immunostaining with RNAscope ISH

Two different combinations, RNAscope and subsequent CODEX as well as CODEX and subsequent RNAscope, were tested. For RNAscope and subsequent CODEX approach, tissue deparaffinization, hydration, antigen retrieval, proteinase digestion, probe hybridization, signal amplification, and development were conducted by following the single RNAscope protocol as described above. After completed the RNAscope, tissue-coverslip underwent CODEX antigen retrieval as described above by following single CODEX protocol. For the CODEX and subsequent RNAscope approach, after the completion of last cycle of CODEX by following the single CODEX protocol as described above, the tissue-coverslip was removed from the CODEX instrument and continued with the single RNAscope procedure from 3% hydrogen peroxide

incubation step on. After the completion of RNAscope procedure, the tissue-coverslip was stained with DAPI (1:2000) for 5 min at RT, washed, and loaded into the CODEX instrument for capturing RNAscope fluorescent image. To integrate RNAscope image to CODEX images, Keyence microscope was set using Keyence software as described above and a new blank cycle was added, where Cy5-channel was assigned to RNAscope. After capturing the RNAscope fluorescent image, image data was transferred into the CODEX file location, where raw data of CODEX plus RNAscope were processed by CODEX processor software.

DISCUSSION

Simultaneous detection of highly multiplexed proteins and RNA in situ is important for understanding health and disease. The spatially resolved relationship of different cells populations, protein and RNA molecules in their native tissue structure bears crucial information for disease diagnosis, pathogenesis and treatment. CODEX represents a powerful new platform for highly multiplexed proteins (up to 60) in situ detection (6, 8, 20). RNAscope represents another power multiplex RNA detection system (up to 12) at a single-copy sensitivity and high specificity (19, 23), where the unique double Z probes and corresponding amplification probes enables concurrent signal amplification and background noise reduction. The combination of RNAscope with regular immunohistochemical or immunofluorescent staining to concurrently detect RNA and protein within the same tissue section has been reported by us (29) and other (30, 31). However, to our knowledge there is no reported study that combined CODEX and RNAscope together. To that end, we tested different combination methods and found CODEX and subsequent RNAscope worked reliably while RNAscope and subsequent CODEX did not work for CODEX signal detection. The following two factors in the RNAscope procedure may damage epitopes for CODEX detection. First, RNAscope uses protease to digest the tissue to facilitate probes access to target sequences. The protease treatment has

been demonstrated to be harsh for many antigenic sites, though some epitopes may survive this treatment (32). Another factor is the dehydration step in the RNAscope method. In a typical protocol, after antigen retrieval, the slide will be dip in ethanol and air dry before adding probes for hybridization. However, preservation immune-recognizable epitopes in tissues requires maintaining a certain amount of water within tissues after antigen retrieval (33, 34). Possible solution for this negative effect of dehydration can be overcome using disaccharides to protect tissue (34) or carefully avoiding tissue drying after antigen retrieval. However, the potential damage some epitopes by protease digestion in a highly multiple protein detection system make this approach not feasible.

For the CODEX and subsequent RNAscope approach, we refined antigen retrieval procedure after finding it was crucial for RNAScope signal detection. Using the hotplate antigen retrieval method is easier to eliminate RNase contamination by baking glass-beaker and coverslip holder. The Comb-CODEX-RNAscope described in this paper can be further enhanced with multiplex RNAscope ISH published recently (35, 36) to maximize the detection of interested RNA signals in addition to highly multiplexed proteins.

The cross-reactivities of 24 CODEX anti-human antibodies to rhesus macaques were also evaluated and 13 were compatible with rhesus macaques. The anti-human CD3 antibody from Akoya did not work for rhesus macaques. Another anti-human CD3 antibody (Clone#: SP162, Cat#: ab245731, Abcam) was conjugated with a barcode-oligonucleotide (Cat#: 5350002, Akoya), which works for rhesus macaque tissues in CODEX.

In summary, a simple and reproducible CODEX and subsequent RNAscope protocol reports here enables spatially resolved highly multiplexed protein and RNA in situ detection, which will facilitate better understanding the health and disease at single cell level in tissue spatial context.

Conflicts of Interest and Source of Funding:

None of the authors in this paper have commercial or other association that might pose a conflict of interest. This work was supported by in part by the NIH R01 AI136756 (Y. Li, Q. Li), R01 DK087625-01 (Li Q), R21 AI143405 (Q Li) and R01AI14503 (W. Hu).

Acknowledgements

Author's contributions: QL and YC designed the experiments. YC conducted most CODEX, RNAscope and combination experiments. RB conducted RNAscope experiments. YC and QL prepared the manuscript and all authors provided manuscript editing. The authors would like to thank Oliver Braubach, Najiba Mammadova and Kristin Schmidt form Akoya for their CODEX technical support. The authors would like to thank the current and previous laboratory members of QL, especially Akoya and Subhra Mandal and Saroj Candra Lohani, for their contribution to rhesus macaque experiments.

REFERENCES:

1. **McGinnis LM, Ibarra-Lopez V, Rost S, Ziai J.** 2021. Clinical and research applications of multiplexed immunohistochemistry and in situ hybridization. J Pathol **254:**405-417.
2. **Parra ER, Francisco-Cruz A, Wistuba, II.** 2019. State-of-the-Art of Profiling Immune Contexture in the Era of Multiplexed Staining and Digital Analysis to Study Paraffin Tumor Tissues. Cancers (Basel) **11**.
3. **Lewis SM, Asselin-Labat M-L, Nguyen Q, Berthelet J, Tan X, Wimmer VC, Merino D, Rogers KL, Naik SH.** 2021. Spatial omics and multiplexed imaging to explore cancer biology. Nature Methods **18:**997-1012.

4. **Parra ER, Zhai J, Tamegnon A, Zhou N, Pandurengan RK, Barreto C, Jiang M, Rice DC, Creasy C, Vaporciyan AA, Hofstetter WL, Tsao AS, Wistuba, II, Sepesi B, Haymaker C.** 2021. Identification of distinct immune landscapes using an automated nine-color multiplex immunofluorescence staining panel and image analysis in paraffin tumor tissues. Sci Rep **11:**4530.
5. **Tsujikawa T, Kumar S, Borkar RN, Azimi V, Thibault G, Chang YH, Balter A, Kawashima R, Choe G, Sauer D, El Rassi E, Clayburgh DR, Kulesz-Martin MF, Lutz ER, Zheng L, Jaffee EM, Leyshock P, Margolin AA, Mori M, Gray JW, Flint PW, Coussens LM.** 2017. Quantitative Multiplex Immunohistochemistry Reveals Myeloid-Inflamed Tumor-Immune Complexity Associated with Poor Prognosis. Cell Rep **19:**203-217.
6. **Kennedy-Darling J, Bhate SS, Hickey JW, Black S, Barlow GL, Vazquez G, Venkataraaman VG, Samusik N, Goltsev Y, Schürch CM, Nolan GP.** 2021. Highly multiplexed tissue imaging using repeated oligonucleotide exchange reaction. European Journal of Immunology **51:**1262-1277.
7. **Schürch CM, Bhate SS, Barlow GL, Phillips DJ, Noti L, Zlobec I, Chu P, Black S, Demeter J, McIlwain DR, Kinoshita S, Samusik N, Goltsev Y, Nolan GP.** 2020. Coordinated Cellular Neighborhoods Orchestrate Antitumoral Immunity at the Colorectal Cancer Invasive Front. Cell **182:**1341-1359.e1319.
8. **Goltsev Y, Samusik N, Kennedy-Darling J, Bhate S, Hale M, Vazquez G, Black S, Nolan GP.** 2018. Deep Profiling of Mouse Splenic Architecture with CODEX Multiplexed Imaging. Cell **174:**968-981 e915.
9. **Giesen C, Wang HAO, Schapiro D, Zivanovic N, Jacobs A, Hattendorf B, Schüffler PJ, Grolimund D, Buhmann JM, Brandt S, Varga Z, Wild PJ, Günther D, Bodenmiller B.** 2014. Highly multiplexed imaging of tumor tissues with subcellular resolution by mass cytometry. Nature Methods **11:**417-422.
10. **Jackson HW, Fischer JR, Zanotelli VRT, Ali HR, Mechera R, Soysal SD, Moch H, Muenst S, Varga Z, Weber WP, Bodenmiller B.** 2020. The single-cell pathology landscape of breast cancer. Nature **578:**615-620.
11. **Angelo M, Bendall SC, Finck R, Hale MB, Hitzman C, Borowsky AD, Levenson RM, Lowe JB, Liu SD, Zhao S, Natkunam Y, Nolan GP.** 2014. Multiplexed ion beam imaging of human breast tumors. Nat Med **20:**436-442.
12. **Keren L, Bosse M, Marquez D, Angoshtari R, Jain S, Varma S, Yang SR, Kurian A, Van Valen D, West R, Bendall SC, Angelo M.** 2018. A Structured Tumor-Immune Microenvironment in Triple Negative Breast Cancer Revealed by Multiplexed Ion Beam Imaging. Cell **174:**1373-1387 e1319.
13. **Gerdes MJ, Sevinsky CJ, Sood A, Adak S, Bello MO, Bordwell A, Can A, Corwin A, Dinn S, Filkins RJ, Hollman D, Kamath V, Kaanumalle S, Kenny K, Larsen M, Lazare M, Li Q, Lowes C, McCulloch CC, McDonough E, Montalto MC, Pang Z, Rittscher J, Santamaria-Pang A, Sarachan BD, Seel ML, Seppo A, Shaikh K, Sui Y, Zhang J, Ginty F.** 2013. Highly multiplexed single-cell analysis of formalin-fixed, paraffin-embedded cancer tissue. Proc Natl Acad Sci U S A **110:**11982-11987.
14. **Hollman-Hewgley D, Lazare M, Bordwell A, Zebadua E, Tripathi P, Ross AS, Fisher D, Adams A, Bouman D, O'Malley DP, Weiss LM.** 2014. A single slide multiplex assay for the evaluation of classical Hodgkin lymphoma. Am J Surg Pathol **38:**1193-1202.
15. **Xu-Monette ZY, Xiao M, Au Q, Padmanabhan R, Xu B, Hoe N, Rodríguez-Perales S, Torres-Ruiz R, Manyam GC, Visco C, Miao Y, Tan X, Zhang H, Tzankov A, Wang J, Dybkær K, Tam W, You H, Bhagat G, Hsi ED, Ponzoni M, Ferreri AJM, Møller MB, Piris MA, van Krieken JH, Winter JN, Westin JR, Pham LV, Medeiros LJ, Rassidakis GZ, Li Y, Freeman GJ, Young KH.** 2019. Immune Profiling and

Quantitative Analysis Decipher the Clinical Role of Immune-Checkpoint Expression in the Tumor Immune Microenvironment of DLBCL. Cancer Immunol Res **7:**644-657.

16. **Lin J-R, Fallahi-Sichani M, Sorger PK.** 2015. Highly multiplexed imaging of single cells using a high-throughput cyclic immunofluorescence method. Nature communications **6:**8390-8390.
17. **Lin J-R, Izar B, Wang S, Yapp C, Mei S, Shah PM, Santagata S, Sorger PK.** 2018. Highly multiplexed immunofluorescence imaging of human tissues and tumors using t-CyCIF and conventional optical microscopes. eLife **7:**e31657.
18. **Saka SK, Wang Y, Kishi JY, Zhu A, Zeng Y, Xie W, Kirli K, Yapp C, Cicconet M, Beliveau BJ, Lapan SW, Yin S, Lin M, Boyden ES, Kaeser PS, Pihan G, Church GM, Yin P.** 2019. Immuno-SABER enables highly multiplexed and amplified protein imaging in tissues. Nature Biotechnology **37:**1080-1090.
19. **Wang F, Flanagan J, Su N, Wang LC, Bui S, Nielson A, Wu X, Vo HT, Ma XJ, Luo Y.** 2012. RNAscope: a novel in situ RNA analysis platform for formalin-fixed, paraffin-embedded tissues. J Mol Diagn **14:**22-29.
20. **Black S, Phillips D, Hickey JW, Kennedy-Darling J, Venkataraaman VG, Samusik N, Goltsev Y, Schurch CM, Nolan GP.** 2021. CODEX multiplexed tissue imaging with DNA-conjugated antibodies. Nat Protoc **16:**3802-3835.
21. **Asp M, Bergenstråhle J, Lundeberg J.** 2020. Spatially Resolved Transcriptomes—Next Generation Tools for Tissue Exploration. BioEssays **42:**1900221.
22. **Schulz D, Zanotelli VRT, Fischer JR, Schapiro D, Engler S, Lun X-K, Jackson HW, Bodenmiller B.** 2018. Simultaneous Multiplexed Imaging of mRNA and Proteins with Subcellular Resolution in Breast Cancer Tissue Samples by Mass Cytometry. Cell systems **6:**25-36.e25.
23. **Atout S, Shurrab S, Loveridge C.** 2021. Evaluation of the Suitability of RNAscope as a Technique to Measure Gene Expression in Clinical Diagnostics: A Systematic Review. Molecular Diagnosis & Therapy doi:10.1007/s40291-021-00570-2.
24. **Hessell AJ, Haigwood NL.** 2015. Animal models in HIV-1 protection and therapy. Curr Opin HIV AIDS **10:**170-176.
25. **Liang B, Li H, Li L, Omange RW, Hai Y, Luo M.** 2019. Current advances in HIV vaccine preclinical studies using Macaque models. Vaccine **37:**3388-3399.
26. **Lu W, Demers AJ, Ma F, Kang G, Yuan Z, Wan Y, Li Y, Xu J, Lewis M, Li Q.** 2015. Next-Generation mRNA Sequencing Reveals Pyroptosis-Induced CD4+ T Cell Death in Early Simian Immunodeficiency Virus-Infected Lymphoid Tissues. J Virol **90:**1080-1087.
27. **Demers A, Kang G, Ma F, Lu W, Yuan Z, Li Y, Lewis M, Kraiselburd EN, Montaner L, Li Q.** 2014. The mucosal expression pattern of interferon-epsilon in rhesus macaques. J Leukoc Biol **96:**1101-1107.
28. **Yuan Z, Wang N, Kang G, Niu W, Li Q, Guo J.** 2017. Controlling Multicycle Replication of Live-Attenuated HIV-1 Using an Unnatural Genetic Switch. ACS Synth Biol **6:**721-731.
29. **Ko A, Kang G, Hattler JB, Galadima HI, Zhang J, Li Q, Kim WK.** 2019. Macrophages but not Astrocytes Harbor HIV DNA in the Brains of HIV-1-Infected Aviremic Individuals on Suppressive Antiretroviral Therapy. J Neuroimmune Pharmacol **14:**110-119.
30. **Annese T, Tamma R, De Giorgis M, Ruggieri S, Maiorano E, Specchia G, Ribatti D.** 2020. RNAscope dual ISH-IHC technology to study angiogenesis in diffuse large B-cell lymphomas. Histochem Cell Biol **153:**185-192.
31. **Kersigo J, Pan N, Lederman JD, Chatterjee S, Abel T, Pavlinkova G, Silos-Santiago I, Fritzsch B.** 2018. A RNAscope whole mount approach that can be combined with immunofluorescence to quantify differential distribution of mRNA. Cell Tissue Res **374:**251-262.

32. **Duncan JS, Elliott KL, Kersigo J, Gray B, Fritzsch B.** 2015. Combining Whole-Mount In Situ Hybridization with Neuronal Tracing and Immunohistochemistry, p 339-352, In Situ Hybridization Methods doi:10.1007/978-1-4939-2303-8_17.
33. **Bolognesi MM, Manzoni M, Scalia CR, Zannella S, Bosisio FM, Faretta M, Cattoretti G.** 2017. Multiplex Staining by Sequential Immunostaining and Antibody Removal on Routine Tissue Sections. J Histochem Cytochem **65:**431-444.
34. **Boi G, Scalia CR, Gendusa R, Ronchi S, Cattoretti G.** 2016. Disaccharides Protect Antigens from Drying-Induced Damage in Routinely Processed Tissue Sections. J Histochem Cytochem **64:**18-31.
35. **Chan S, Filezac de L'Etang A, Rangell L, Caplazi P, Lowe JB, Romeo V.** 2018. A method for manual and automated multiplex RNAscope in situ hybridization and immunocytochemistry on cytospin samples. PLoS One **13:**e0207619.
36. **Xiao L, Labaer J, Guo J.** 2021. Highly Sensitive and Multiplexed In Situ RNA Profiling with Cleavable Fluorescent Tyramide. Cells **10**.

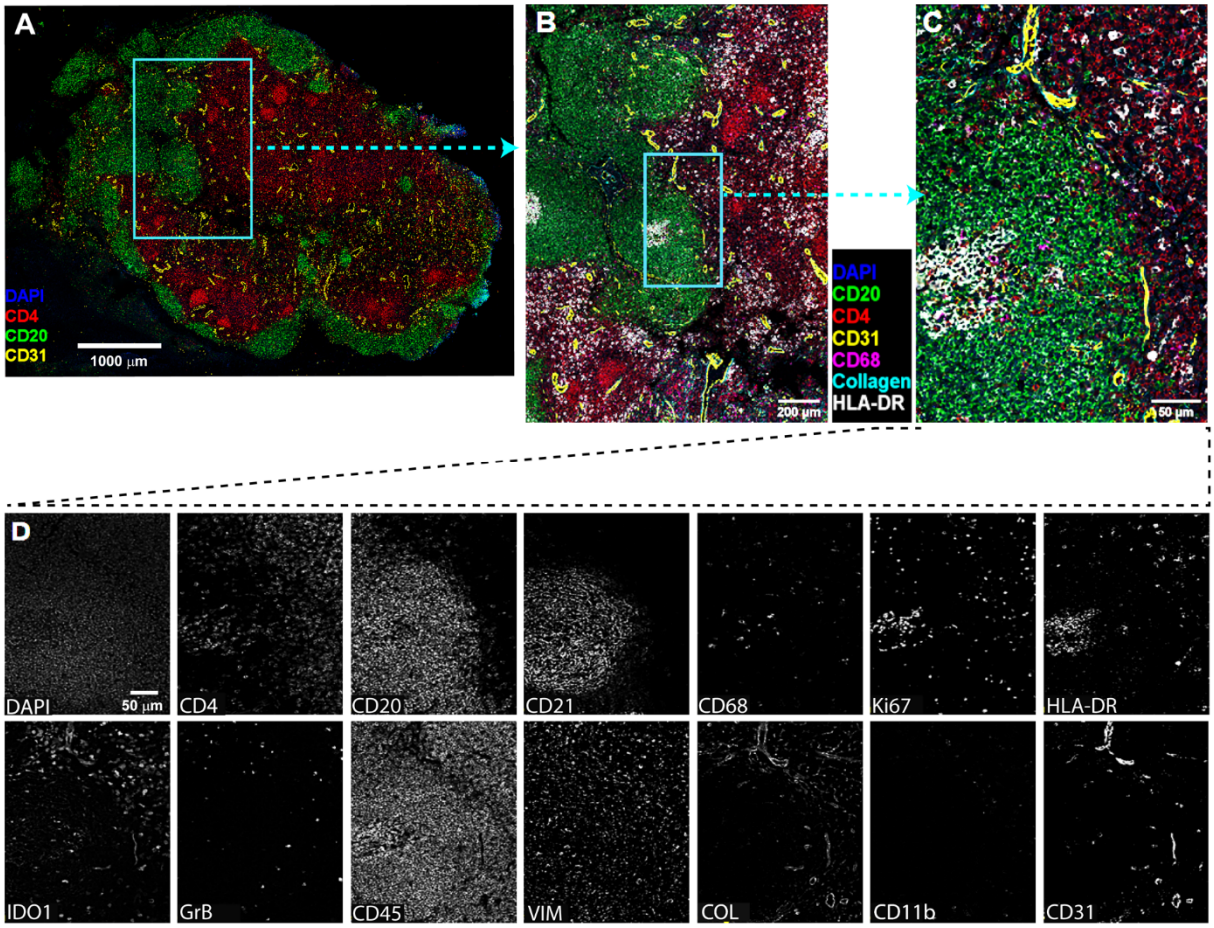

Figure 1. The cross-reactivities of 24 DNA-barcoded anti-human antibodies from Akoya to rhesus macaques using CODEX. (**A**) Overview image of lymph node tissue from a rhesus macaque infected with SIVmac251 (Rh4979, 10 dpi), showing CD4 (red), CD20 (green), DAPI (blue) and CD31(yellow). (**B**) The boxed area in A was zoomed to show DAPI (blue), CD4 (red),

CD20 (green), CD68 (magenta), Collagen (cyan), HLA-DR (white) and CD31(yellow). (C) The boxed area in B was zoomed. (**D**) individual channel image showing 13 cross-reactive anti-human antibodies to rhesus macaque. Scale bars are shown

Table 1. The cross-reactivities of CODEX anti-human DNA-Barcoded-antibodies from Akoya to rhesus macaques

Antibody	Clone#	Cross-reactivity to rhesus macaque
CD107a	H4A3	+
CD11c	A118/A5	-
CD14	EPR3653	-
CD20	L26	+
CD21	EP3093	+
CD31	EP3095	+
CD3e	EP449E	-
CD4	EPR6855	+
CD44	156-3C11	-
CD45	D9M81	+
CD45R0	UCHL1	-
CD11b	EP1345Y	+
CD68	KP1	+
CD8	C8/144B	-
CollagenIV	EPR20966	+
E-Cadherin	4A2C7	-
Granzyme B	D6E9W	+
HLA-DR	EPR3692	+
Pan-Cytokeratin	AE1/AE3	-
IDO-1	V1NC3IDO	+
Vimentin	O91D3	+
CD57	HNK-1	-
CD34	QBEND/10	-
Ki67	B56	+

393

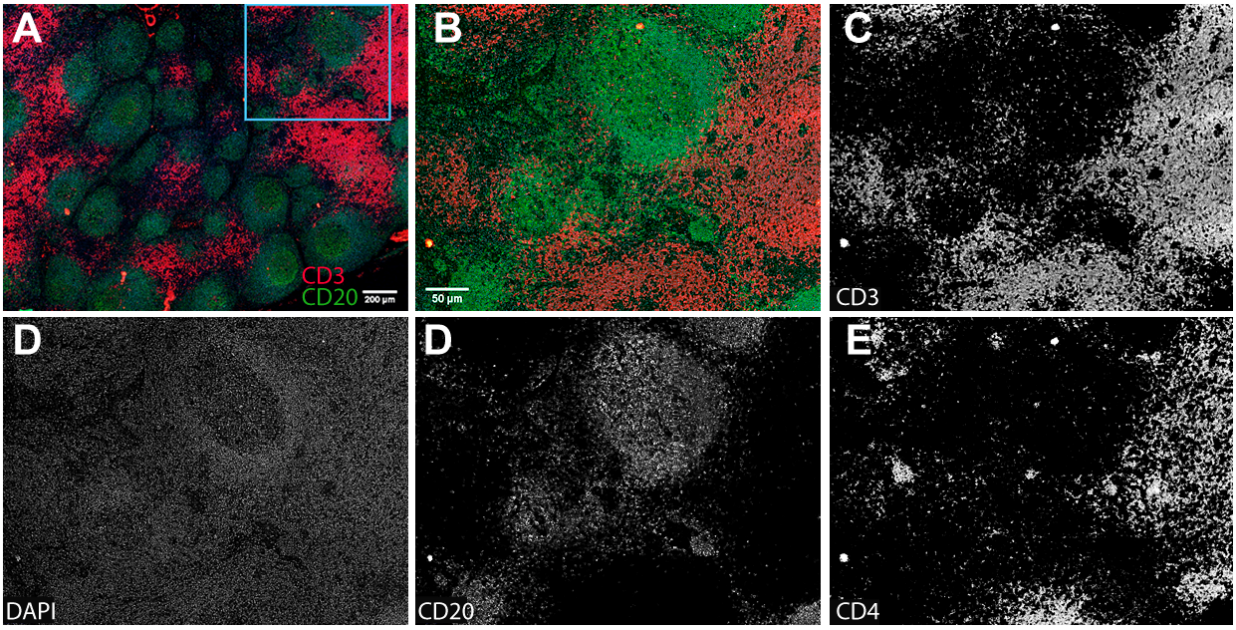

Figure 2. Validation of a home anti-human CD3 antibody (SP162, Cat#: ab245731, Abcam) conjugated with a DNA-barcode using CODEX to rhesus macaques. (**A**) Overview image of lymph node tissue from a rhesus macaque infected with SIVmac251 (Rh4979, 10 dpi). (**B**) The boxed area in A was zoomed. (**C-E**) individual channel image of antibodies, showing CD3, CD20, CD4 and DAPI. Scale bars are shown

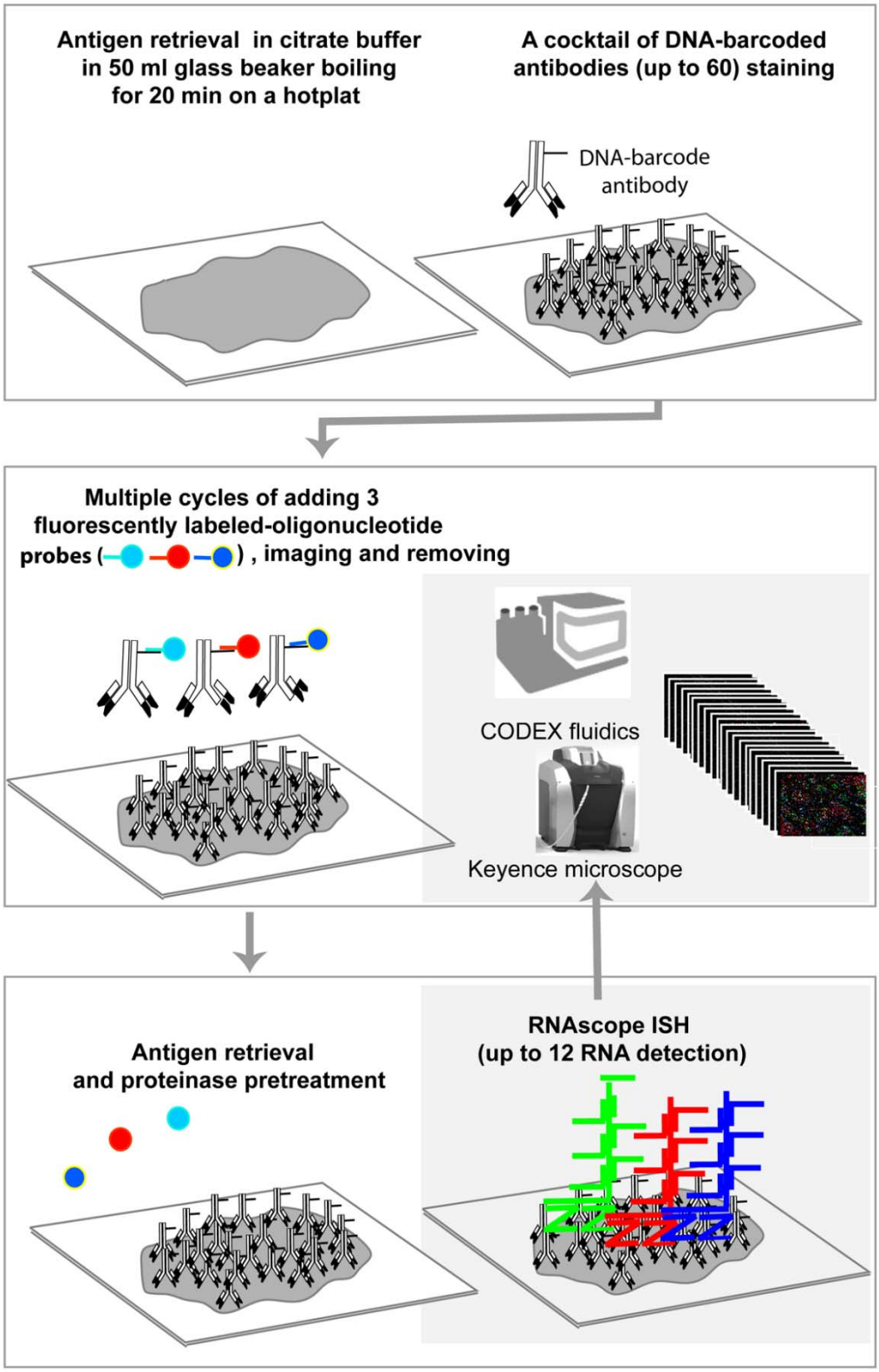

Figure 3. The workflow of CODEX and subsequent RNAscope in situ hybridization combination (comb-CODEX-RNAscope).

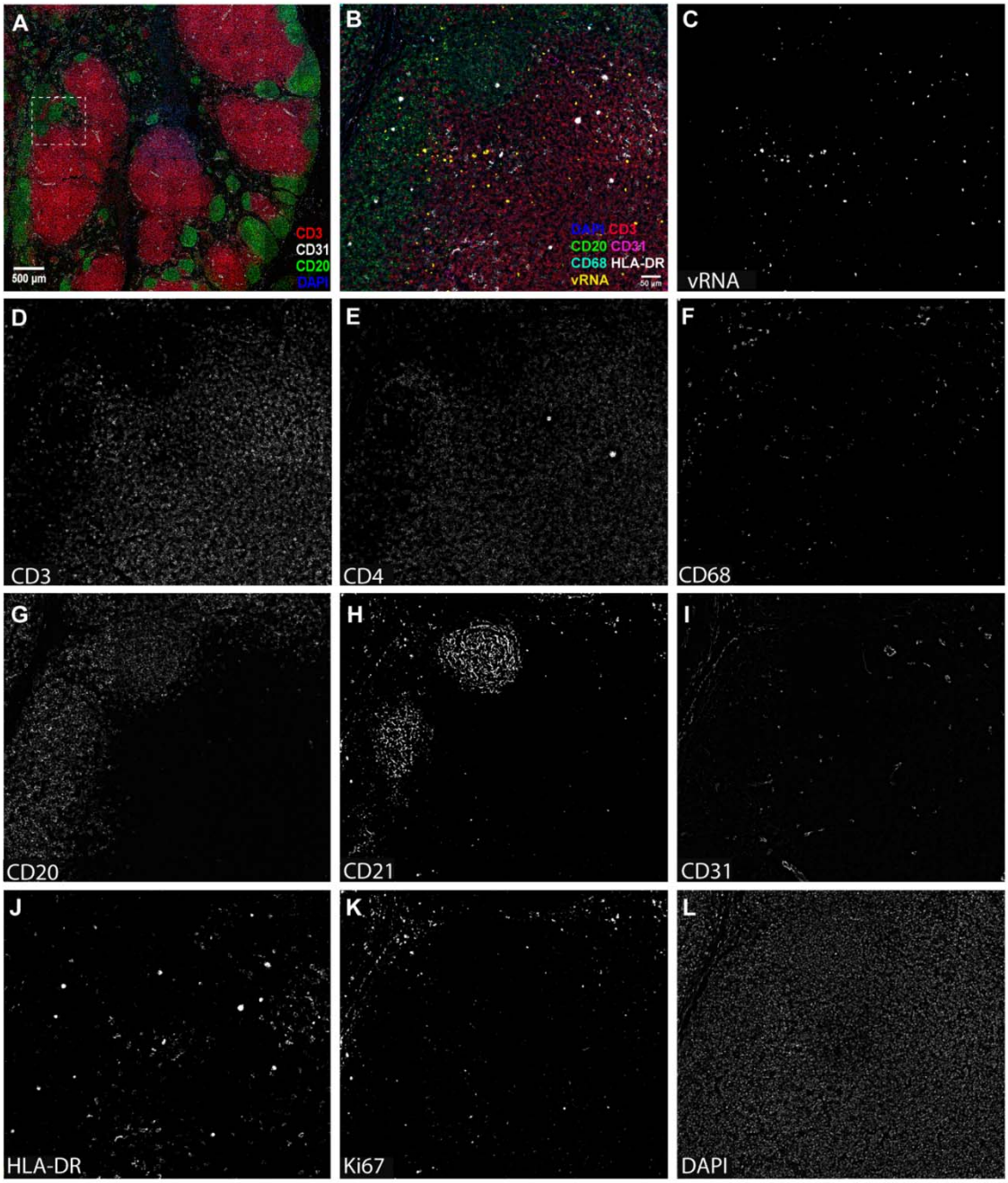

Figure 4. Representative images of the comb-CODEX-RNAscope. (**A**) Overview image of lymph node tissues from a rhesus macaque infected with SIVmac251 (Rh4979, 10 dpi), showing CD3 (red), CD20 (green), CD31(white) and DAPI (blue). (**B**) The boxed area in A was zoomed to show SIV viral RNA detected by RNAscope and other 5 protein markers by CODEX. (**C-L**) individual channel image showing vRNA and protein biomarkers. Scale bars are shown.